Article

An Analytical Model for Estimating Ship-Related Emissions in Port Areas

Filip Bojić *, Anita Gudelj [ID] and Rino Bošnjak [ID]

Faculty of Maritime Studies, University of Split, 21000 Split, Croatia; anita@pfst.hr (A.G.); rinobo25@pfst.hr (R.B.)
* Correspondence: fbojic@pfst.hr

Abstract: Intensive shipping activity in port areas is considered one of the leading problems in the maritime sector, which has a negative effect on climate change and local air quality. The compilation of detailed inventories of combustion gases released by ships should therefore provide a more accurate overview of emission levels, which can serve as a basis for analysing impacts on the port community and lead to the establishment of better environmental measures. Thus, the aim of this study was to develop an adaptable and relevant analytical model capable of integrating a comprehensive methodology with large databases of ship movements and technical details to provide clear ship-related emission estimates in large port areas. Considering the lack of research in Croatia that includes the mentioned approach and the insufficient monitoring of air pollutants in ports, the model was used to produce an initial overall emissions inventory for the Port of Split, the busiest passenger port in Croatia. In the model, bottom-up logic with an energy-based method was applied to detailed technical and near-real-time shipping data from AIS, creating the first high-density spatial and temporal overview of shipping emissions in the City port basin. The results showed strong seasonal fluctuations and large discrepancies in the quantities emitted between different ship types and operating modes. The analysis therefore raised the question of the need for the future development and implementation of a scalable system that would provide a more transparent and efficient overview of the important characteristics of air pollution from ships and port areas.

Keywords: ship emissions; air pollution modelling; AIS; environment; Port of Split

1. Introduction

Although shipping is widely recognised as the most sustainable mode of transport since large volumes of cargo can be carried in a single trip, extensive quantities of marine fuels are used for propulsion during transportation [1–4]. The internal processes of energy conversion and combustion in ship engines mainly produce air pollutant substances (APSs) such as sulphur oxides (SOx), nitrogen oxides (NOx), particulate matter (PM), carbon monoxide (CO), and volatile organic compounds (VOC), as well as carbon dioxide (CO_2), methane (CH4), and nitrous oxide (N2O), recognised as greenhouse gases (GHGs) [1,5–7]. While anthropogenic GHGs are responsible for global warming and the adverse effects of climate change, other air pollutants released from fuel combustion have serious impacts on human health in urban areas [1,7,8]. It was documented that exposure to the PM2, SOx, NOx, CO, and VOC is associated with respiratory illness, cardiovascular disorder, lung cancer, and premature mortality [8,9]. Given that 70 to 80% of world trade is seaborne, maritime transport contributes significantly to anthropogenic emissions [1,3].

Aiming to reduce ship-sourced air pollution, the International Maritime Organisation (IMO), in 1997, extended the MARPOL convention with Annex 6 "Prevention of Air Pollution from Ships". The main objective of the entry into force of MARPOL Annex 6 was to mitigate SOx, NOx, VOC, and PM emissions by establishing stringent fuel quality and emission control regulations applicable to ships and Emission Control Areas (ECAs) [10]. Under the revised MARPOL Annex 6, the global sulphur limit is reduced to 0.50% mass

by mass percent (% m/m), effective from 1 January 2020, while the content in ECAs is reduced to 0.1% m/m [10]. Progressive reductions in NO_x emissions from marine diesel engines is regulated through a three-tier system. The less rigid Tier 1 applies to ships built on or after 1 January 2000, Tier 2 for ships built on or after 1 January 2011, while the most demanding Tier 3 regulates NOx emissions from ships built after January 2016, or 2021, and operating in ECAs [10]. It is expected that the measures for SOx and NOx should also reduce the quantity of PM and VOCs released into the atmosphere. Regarding the mitigation of GHGs, the IMO added a new Chapter 4 to MARPOL Annex 6, which provides two important measures. In the first one named the Energy Efficiency Design Index (EEDI), it is required for new ships to comply with minimum mandatory energy efficiency performance levels, increasing over time through different phases [11]. The Ship Energy Efficiency Management Plan (SEEMP) is an operational measure that establishes a mechanism to improve the energy efficiency of a ship in a cost-effective manner [11].

However, regardless of the numerous revisions to MARPOL Annex 6 and the continued application of more stringent emission control regulations, the IMO has recorded an increase in overall GHG air pollution from ships [12]. It was noted that, from 2012 to 2018, emissions of CO_2, NOx SOx, PM, CO, VOC, and CH4 increased by 5.6%, 1.2%, 5.5%, 3.5%, 10.2%, 7.6%, and 151%, respectively [12]. This rise of ship-related air pollutant volumes released into the atmosphere is mostly connected to the growth rates of fuel consumption due to increased shipping demand [12]. Although overall carbon intensity has improved by 20–30% over the same period, the study also stated that it will be difficult to achieve the IMO's GHG reduction goal of 50% by 2050 [12]. Therefore, countries should anticipate, prepare for, and adapt to climate change by fully understanding the risks, exposure, and vulnerabilities [13].

With the same tendency, but focusing on the regional aspect, the European Sea Ports Organisation (ESPO) has recognised the problems of air quality, climate change, and energy efficiency in the port sector of the European Union (EU) as three of the most important environmental priorities [14]. Ports account for a small share of global maritime traffic emissions, but their function as major transport hubs leads to intensive shipping activity and thus to a corresponding emission of air pollutants. Port-related emissions from ships engines have strong spatial and temporal significance that directly affects air quality in port communities. Considering that 90% of European ports are spatially connected to cities, the magnitude of air quality degradation is even more serious [14,15].

Although all EU countries are required to monitor their emissions under the EU Climate Monitoring Mechanism, and the European Environment Agency (EEA) compiles national inventories in accordance with the Intergovernmental Panel on Climate Change (IPCC) guidelines, emissions from maritime transport, particularly in port areas, are still vague in some regions [16–18]. An example of unclear monitoring of air pollution from shipping can be observed in Croatia. In the latest Croatian GHG inventory, general fuel consumption (Tier 1 method) was applied to estimate emissions from navigation, but without spatial, temporal, or technical details [19]. The Croatian part of the Adriatic coast is 1777 km long and has six ports of international economic importance open to public traffic, where most of the 359,223 arrivals of various types of ships were recorded in pre-pandemic 2019 [20,21]. Thus, it is necessary to obtain a better insight into air pollution from the maritime sector, especially in port areas with large communities [4,22–24]. Moreover, emission inventories should quantify not only GHG but also other pollutants that may compromise the health of the port-city population.

That is why the importance of high-resolution shipping emission inventories for port areas is recognised by both the port and scientific communities [14,15,23–27]. The results of a detailed air pollution study should reveal more accurate emission levels that can be used as a basis for analysing impacts on the port community, leading to the establishment of better environmental measures. However, to calculate quantities of air pollutants with higher accuracy, a bottom-up energy-based method should be applied on large datasets that contain relevant shipping information. IMO Regulation V/19, which requires the

installation of an Automatic Identification System (AIS) on merchant ships of 300 GT (GT) and all passenger ships, has made near real-time data on ships and their movements available [1]. Accordingly, an increase in bottom-up energy-based gas emission inventories for ports has been noted, suggesting that by combining high-resolution data with the appropriate methodology, it is possible to obtain coherent estimates of air pollution from ships in ports [15]. The systematic review showed that the bottom-up approach was used frequently in papers analysing ship-related emissions in 80 different ports, with the energy-based method being predominantly applied [15]. However, as bottom-up approach requires large databases, calculating emissions is a complex and time-consuming operation, especially when estimation is not systematically processed.

Therefore, the focus of this research was to develop an adaptable and relevant analytical model capable of integrating a comprehensive methodology with large amounts of shipping data to produce clear ship-related emission estimates in large port areas. Considering the lack of research in Croatia that includes the mentioned approach and the insufficient monitoring of air pollutants in ports, the model was used to develop an initial overall emissions inventory for the Port of Split, the busiest passenger port in Croatia. The inventory with high temporal-spatial resolution can be used as a basis for developing strategies to control emissions. In the model, the bottom-up approach and the energy-based method were applied to detailed technical and near-real-time shipping data from the AIS to calculate levels of air pollutants released by ships in the City port area. Throughout the three-step process, estimates of CO_2 and CH4 as GHGs and SOx, NOx, PM10, PM2.5, NMVOC, and CO as APSs were determined on a ship-by-ship basis for the entire year of 2019. Exhaust gas volumes with relevant data on the production of air pollutants from marine engines are stored and can be handled by the model to generate various analytical results. The model was therefore able to produce a novel, high-density, activity-based ship emissions spatial distribution map, together with a detailed overview of technical, temporal, and operational aspects. In addition, a unique differentiation of ship types was developed to ensure proper and effective imputation of missing data while providing the background for a future extension of the model's predictive capabilities.

2. Materials and Methods

The methodology for estimating ship-sourced gas emissions in port areas applied in this research is based on a comparative analysis of relevant papers and studies within the PRIMSA approach and meets the requirements of the IPCC guidelines [15]. The mentioned paper stated that the bottom-up energy-based methodology is most reliable for estimating ship-sourced gas emissions in port areas since it requires a high level of input parameters [15,23]. Since this approach enables calculation on a ship-by-ship basis by combining energy output with emission factor (EF) and time, large databases that contain specific technical data on the ships and detailed information on movement activities need to be used. Static technical data on the details of the ships and their engines describe components for the emission calculations, such as main/auxiliary engine power ($P_{ME/AE}$), engine function, engine type, and fuel type [15]. Dynamic data on ship MA is categorised by the operational mode of the ship's propulsion and generator systems and defined by the percentage of ME and AE working load expressed as LF [15]. Considering that the specific workload of the engines has a direct influence on the emission production, the time spent in cruising, manoeuvring, and hoteling activities must be taken into account. As the central and most complex segment of the emissions quantification process, EF depends on both static data on engine function, speed, engine type, and fuel type and dynamic information on the characteristics of the ship's activities [15]. Therefore, the bottom-up energy-based methodology expressed in Equation (1) that contains key factors proposed in the systematic review is implemented in the emission estimation model presented within Figure 1 [15].

$$E = (P_{ME} \times LF \times EF_{ME} + P_{AE} \times LF \times EF_{AE}) \times T \times CF \qquad (1)$$

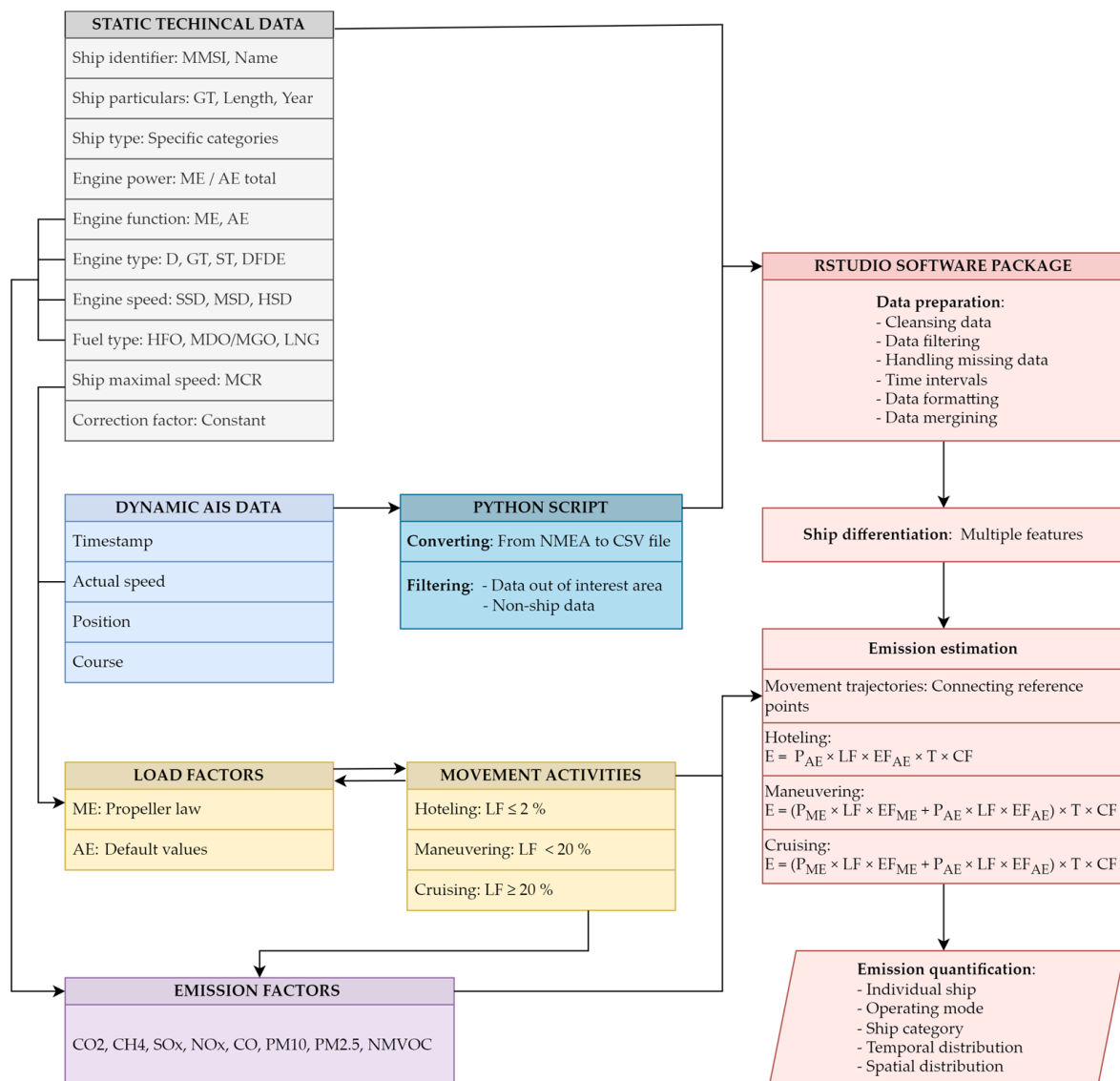where the following definitions apply:

Figure 1. Flow diagram of the model for estimation of ship emissions in port areas.

E: E missions quantity by mode for each ship call—in grams (g);

$P_{ME/AE}$: total power of main engines/auxiliary engines—in grams per kilowatt hour (g/kWh);

LF: load factor expressed as actual engine work output—as a percentage of engine power (%);

$EF_{ME/AE}$: emission factors of different pollutants in regard to engine function, engine type, fuel type, and installation year—in grams per kilowatt hour (g/kWh);

T: time spent in a certain movement activity—in hours (h);

CF: correction factor for emission reduction technologies—constant.

The model for ship-related emissions estimation in ports has three complex and interconnected phases. In the initial preprocessing stage, data collection was carried out with recourse to several databases. The data from AIS had to be cleaned and converted from 'raw' format into a readable comma-separated values (CSV) file in order to be merged, filtered and structured together with the static technical data. Methods for ship type differentiation and emissions estimation were then applied on formatted technical and activity data as a part of the processing phase. Lastly, in the postprocessing phase, output data was stored and handled, aiming to create spatial and temporal visualisations of shipping emissions.

The dynamic AIS data was transferred through Python, while the handling and analysis were carried out using the RStudio 2023.09.1+494 software package. Within the grey box that contains technical features, MMSI stand for Maritime Mobile Service Identity, GT for gross tonnage, D for diesel engine, GTU for gas turbine, STU for steam turbine, DF for dual fuel, SS/MS/HS D for slow-/medium-/high-speed diesel engine, HFO for heavy fuel oil MDO/MGO for marine diesel/gas oil, LNG for liquified natural gas, and MCR for maximum continuous rating. MCR is defined as the manufacturer's tested engine power [28]. Usually, a ship operates at the nominal continuous rating, which is 85% of the 90% of MCR [26]. Inside the dark blue box, NMEA stands for National Marine Electronics Association sentence format.

Considering that the aspects of the main data processing components of the model are based on universal characteristics that have a significant effect on the production of air pollutants, it can be concluded that the model is not restricted to one case study and can be applied to different ports. Also, the flexibility of the model structure allows the inclusion of new insights and other aspects relevant to the port-based shipping emissions, expanding the quality and scope of the final output.

It is important to add that large quantities of technical data have enabled a specific differentiation of ship types based on the analysis of multiple characteristics. This feature allowed for more accurate and effective missing-data imputation and provided a basis for future expansion of the model's capabilities in emissions forecasting and scenario building.

2.1. Maritime Traffic, Spatial and Temporal Specifications

To determine the exact databases for the emission calculations, the temporal, spatial, and transportation characteristics of the research area must first be defined and analysed. As it was stated, the modelling of emissions was conducted by relying on historical data on shipping traffic in the Port of Split—City port basin in 2019.

The Port of Split is one of the busiest ports in the Mediterranean in terms of passenger and vehicle traffic, while cargo traffic remained within the bounds of local importance. For example, in 2019, the busiest year on record, 5,607,789 passengers and 829,594 vehicles were transported, but only 2,913,509 tonnes (mt) of cargo was transferred [29]. The distribution of maritime traffic is thus almost exclusively concentrated on various types of passenger ships, mainly Ro-Ro ferries, high-speed craft, cruise ships, and pleasure craft, which account for almost 90% of arrivals.

Spatially, the Port of Split is divided by the city of Split into two dislocated areas. One area, called North port, is situated on the northern side of the Split peninsula and consists of several basins, mainly for cargo ships. City port basin forms the second part of the port, which is intended for passenger ships and where, on average, about 90% of all maritime traffic is handled. The City port is located in the southern part of the Split peninsula, where it is spatially and infrastructurally integrated into the city centre, what can be seen in Figure 2. Due to the locational connection with the urban environment, high traffic density of City port and the fact that Split is the second most populated Croatian city, air degradation can represent a serious threat to public health. The city's connection with the Adriatic islands and the Apennine Peninsula via numerous shipping lines and its popularity as a cruise and tourist destination with a growth trend further emphasises the need for monitoring and control of pollutants from maritime traffic. Thus, this study focuses on the area of the City port with the aim of estimating and analysing ship-induced air pollution. The research area with the relevant coordinates is shown in Figure 3. The dynamic AIS data was transferred through Python, while the handling and analysis were carried out using the RStudio software package (https://www.r-studio.com/data-recovery-software/).
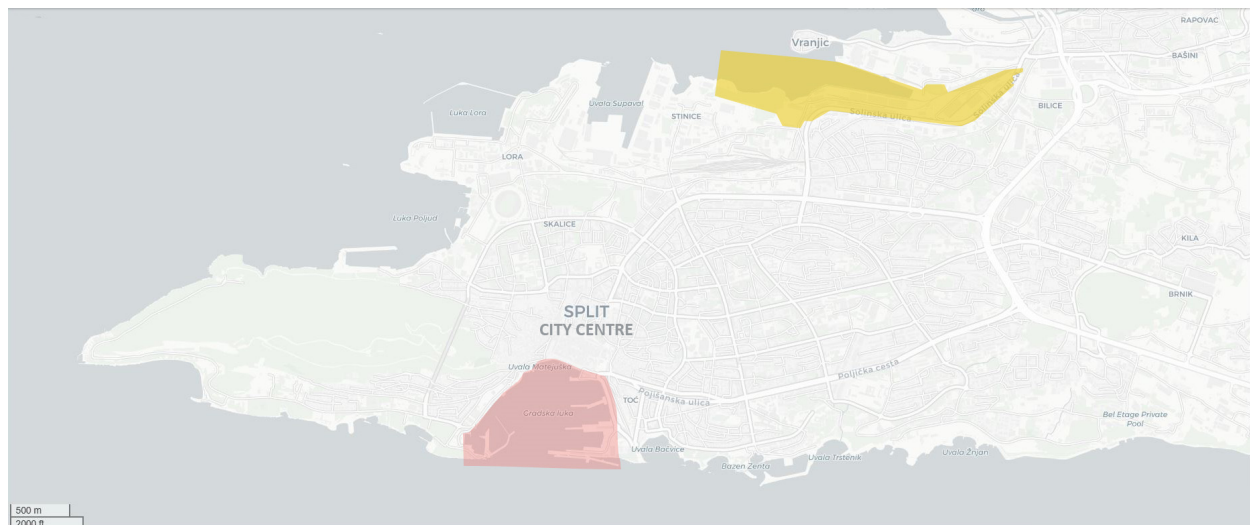
Figure 2. Overview of Port of Split basins and Split city centre.
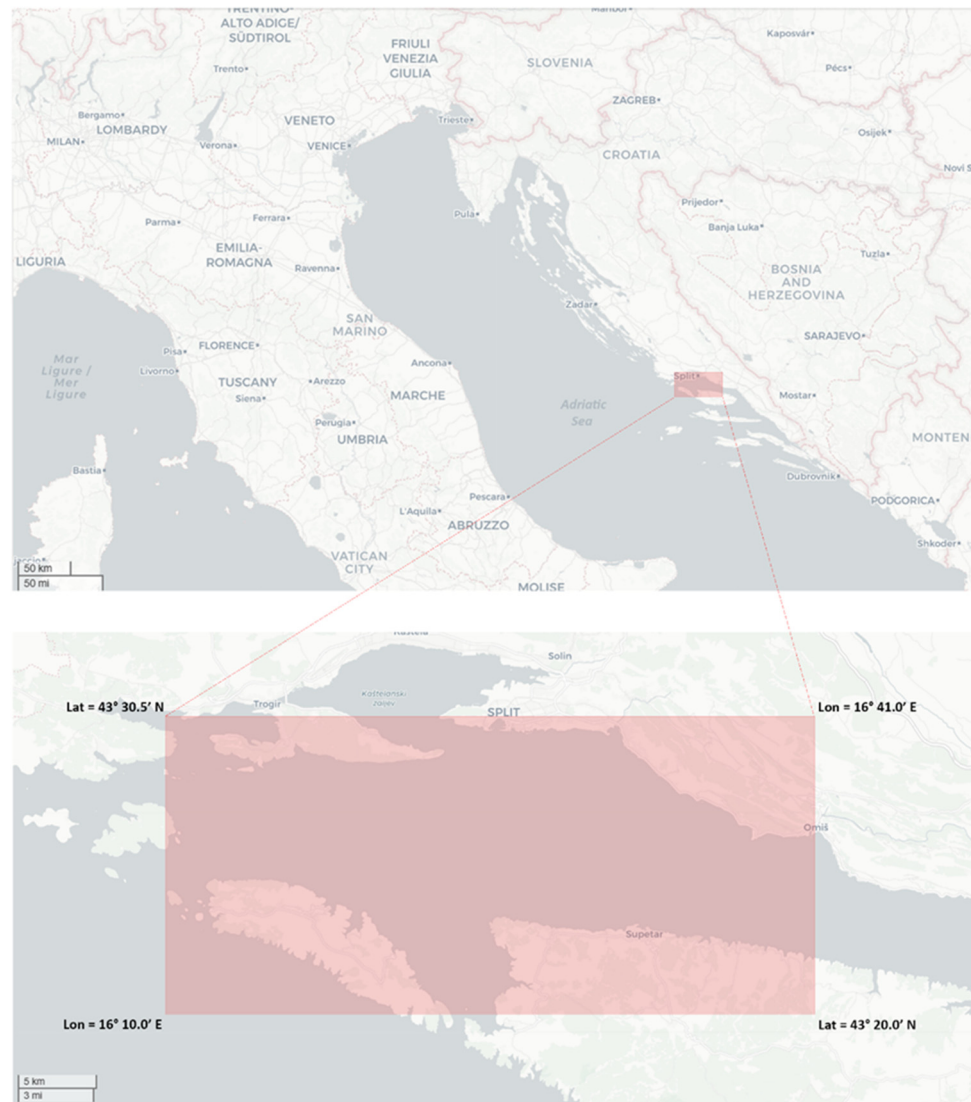

Figure 3. Research area in relation to the region with respective geographic coordinates.

Part of the area of the North port is marked in yellow, while the City port basin is in red. The grey area in between represents the urbanised parts and the locational connection of the City port with the town centre. Note: the map was generated with the RStudio software package and then modified.

2.2. Defining Input Databases—Technical Data and Activity Data

Based on the name, type, and MMSI number as identifiers, a database of technical information about ships and their engines was created by collecting attributes from the Croatian Registry of Shipping (CRS), the Croatian Integrated Maritime Information System (CIMIS), and web data (WD) from relevant shipping companies. Gathered data refers to GT, length, breadth, year, MA power, AE power, engine type, engine speed, fuel type, maximal speed at MCR, and relevant emission mitigation technology. Considering that several data sources were used, it was possible to corroborate mentioned information, and where data was redundant, the CRS database was prioritised.

The primary function of AIS is to ensure higher level of navigational safety by sharing timely information on ship characteristics and their movement between other vessels and the shore [30]. However, both static and dynamic data transmitted by AIS provide a detailed overview of ship movements and their characteristics, which is more often applied in emission estimation process [15,23]. Therefore, the AIS database that contains relevant shipping data applied in this research was provided by the Faculty of Maritime Studies in Split. Generally, the static data broadcasted through AIS refers to MMIS number, IMO number, ship type, length, name, and call sign [31,32]. Dynamic data on ship movement reveals the position of the ship, the timestamp, the course over ground (COG), and the speed over ground (SOG) [30,32]. As the AIS dataset does not contain all features required for the estimation of emissions, such as engine details or LF, only dynamic data was used, while static information represented by the above identifiers was included in the data merging process.

2.3. AIS Dataset Conversion and Filtering

A prerequisite for the integration of technical information with activity details is the conversion of the AIS data. AIS operates in the very high frequency (VHF) mobile maritime band or uses satellite communication for broadcasting messages in NMEA sentence format [33]. NMEA files are in 'raw' encoded form and as such are not readable by statistical data processing software. Therefore, a specific Python script was developed and integrated inside the model to convert the 'raw' data from AIS into a readable CSV format. Considering that the use of AIS is not limited to ships nowadays and that the AIS station used in this research covers a larger area than necessary, both spatial and non-ship filters were included in the script. As a final result of the AIS data preparation, timestamps with current speed, position, and course were extracted together with the corresponding identifiers for each transmitted point of each vessel that passed through the selected area in 2019. Since AIS generally generates and shares data every few seconds, 71,638,920 entries were obtained and taken into account for further preparation. Although processing a database of this size is very time-consuming and computationally intensive, it provided the basis for identifying emissions with high spatial and temporal density.

2.4. Data Preparation

In the last step of the preprocessing phase, the RStudio software package was used to develop code that enabled the cleansing, filtering, formatting, and merging of data. Cleansing was applied on AIS datasets, aiming to exclude duplicate and faulty data. In this process, entries missing identifiers and/or all particulars were screened out. Ships that passed through the interest area but did not arrive at the designated port basin were filtered out. The same principle was applied to the entries or the entire movement tracks with abnormal values for speed (more than 40 kt), position, and/or time. After eliminating inadmissible datasets, 49,540,895 entries were used for the research. Given that

the technical and activity datasets were collected from several sources, their structure had to be formatted to establish a standardised form. Once a consistent display of the cleansed and filtered data was achieved, the specific technical details of each vessel were merged with all corresponding activity entries recorded in 2019 by linking the unique identifiers. Performing all the mentioned steps of the preprocessing phase within the model enabled emission estimation on a ship-by-ship basis, but also the implementation of the specific differentiation of ship types.

2.5. Ship Types Differentiation and General Characteristics

The two main functions of differentiating ship types based on the analysis of multiple characteristics are to ensure more accurate and effective imputation of missing data while also providing a basis for future expansion of the model's capabilities in emission forecasting and scenario building. Although AIS datasets already contain predefined information on ship type, their characteristics can vary considerably. This refers in particular to the ship's dimensions (GT, length), the MCR speed, engine details (power, type, speed), and also to the function of the ship. Thus, the ship type differentiation had to be performed in two steps.

Throughout the analysis of AIS datasets, it was found that most ship types were categorised in general terms (e.g., passenger, cargo, tanker, fishing) without additional information on the function of the ship (cruise ship, Ro-Ro, ferry, etc.). Therefore, as a first step, the ships were divided into specific groups according to their main function. However, large oscillations in technical and engine details were found in some categories. A good example is to compare two cruise ships, one of which had 2995 GT and an ME power of 2460 kW, while the other had 90,940 GT and an ME power of 50,000 kW. To create categories of ships with similar technical characteristics, certain types of ships were differentiated by applying the probability distribution to multiple characteristics that showed significant fluctuations. As a result of the second step, 11 specific ship types were identified based on the collected data:

- Large cruise ships;
- Medium cruise ships;
- Small cruise ships;
- Large Ro-Ro ferries;
- Ro-Ro ferries;
- High-speed craft;
- Excursion ships;
- Fishing;
- Tug;
- Pleasure craft;
- Sailing.

By subdividing categories of ships, it was possible to perform more specific and effective missing-data imputation. In this process, average values from corresponding group of ships were assigned to the features where data was missing. After operating the model, the imputed data displayed low level discrepancy, which allows for a more accurate estimation of emissions, even when all data is not available.

2.6. Emissions Estimation

In the last step of the processing phase, the model uses bottom-up logic where reference points are combined into specific movement trajectories to calculate the complete amount of air pollutants emitted during individual visits to the port basin for each ship included in the study. This way, the model is able to produce detailed estimates for each individual ship with high temporal and spatial density by applying the energy-based emission estimation method. However, throughout the port approach and departure operations, ships have to alter their speed, which leads to a change in the energy output of the engines, and consequently, to a trend in the production of air pollutants. Therefore, in order to estimate

emissions based on energy demand, the operating modes with the time spent in them were determined for each trajectory.

2.6.1. Estimation of the LFs and Operating Modes

It is generally accepted that different rates of engines working load have direct impact on internal combustion processes that are responsible for releasing air pollutants into an atmosphere [12,34]. Some studies suggest that engines are the most efficient when operated at around 80% load and are not as efficient at lower loads. This applies in particular to LF of less than 20%, which are normally achieved when ships are preparing to berth or depart and are manoeuvring at low speed. Due to the mentioned low-load effect on engine efficiency, the model recognises three distinct modes of operation: cruising, manoeuvring, and hoteling. As the cruising mode is identified by engine loads above 20% and manoeuvring is defined with LF values that are lower, hoteling operation is considered when the ships have switched their ME off and only use the generators while at berth or at anchor. Since the load of the ME correlates with the speed, the collected AIS and technical data were used in the propeller law method expressed in Equation (2) to estimate LF and define the related operating modes for each trajectory, while the corresponding timestamps were used to calculate the operating time [12,34].

$$LF = (S_A / S_M)^3 \tag{2}$$

where the following definitions apply:

S_A: actual speed of the ship—in knots (kt);

S_M: speed of the ship at MCR—in knots (kt).

Although the workload of the ship's generators corresponds to the specific power requirements of the operating modes, it is not possible to anticipate it through the propeller law or similar methods, which is why the LFs of the AEs are generally vague [22–27]. In the absence of a specific study on AE workloads on ships navigating within the area of interest, static LF values from several large-scale studies and papers with similar traffic and spatial specifications were used [4,17,34].

2.6.2. Estimation of the EFs

As was stated, energy conversion in marine engines is a complex process with a number of variables that directly affect the production of air pollutants and may vary for different gases. Therefore, to calculate exact EFs for particular engines and the fuel they consume in specific operation modes, onboard measurements should be carried out, which requires specific research to be conducted on this topic. Since such studies are financially and logistically costly, the identification of the EFs is the vaguest area in the emission estimation process [12,15,22,23,25–27]. Therefore, in this study, collected technical data was combined with the estimated operating modes in comprehensive methods to determine the corresponding EF and connect them to the relevant reference points. The components used for identifying EFs are listed in Table 1, while the low-load adjustment values for all gases (except for NOx) included in the study were taken from the San Pedro Bay Ports Report and applied when the ships were operating in manoeuvring mode [34].

Table 1. Technical data and operating modes included in the model for EF identification.

EF Components					
Engine Function	Engine Type	Engine Speed (rpm)	Fuel Type	Mode and LF	
ME	D	SS D < 300	MDO/MGO	Cruising	LF ≥ 20%
AE	GTU	MS D 300–900	HFO	Manoeuvring	LF < 20%
	STU	HS D > 900	LNG	Hoteling	LF ≤ 02%
	DF				

Emissions of CO_2 and SOx are directly proportional to fuel consumption. Thus, specific fuel consumption (SFC) load was calculated by applying the method from the third IMO GHG study and baseline values from the recent fourth IMO GHG study, as is shown in Equation (3) [12,35].

$$\text{SFC load} = \text{SFC baseline} \times (0.455 \times LF^2 - 0.71 \times LF + 1.28) \tag{3}$$

where the following definitions apply:

SFC load: SFC at a given engine load—grams of fuel consumed per kilowatt-hour (g/kWh);

SFC baseline: efficient SFC for a particular engine—engine load optimised at 80%.

After determining the SFC of engines under optimal and low-load conditions by applying LF values from 0 to 1, it was possible to determine CO_2 and SOx EF based on fuel usage. However, since the model developed in this study uses an energy-based logic, the methods presented in the fourth GHG study for calculating the EF for the mentioned gases had to be modified. For CO_2, a non-dimensional conversion factor (Cf) measured in g of CO_2 emitted per g of particular fuel consumed was taken from the MEPC.308(73)—2018 EEDI Guidelines [36]. As the Cf corresponds to the fuel used when determining SFC, Equation (4) was established to transfer the CO_2 EF from a fuel- to energy-based measure.

$$CO_2\ EFe = SFC \times EFf \tag{4}$$

where the following definitions apply:

EFe: energy-based emission factor—grams of pollutant emitted per kilowatt-hour (g/kWh);

EFf: fuel-based emission factor equal to Cf—grams of pollutant emitted per g of fuel consumed (g pollutant/g fuel).

As an air pollutant, SOx emissions vary with the sulphur content of the fuel and accordingly to fuel consumption. Therefore, Equation (5) presented in the fourth GHG Study was combined with Equation (4) to convert EFf of SOx to Efe [12].

$$SOx\ EFf = 2 \times 0.97753 \times S \tag{5}$$

where the following definitions apply:

S: sulphur content of a particular fuel — grams of pollutant per g of fuel (g pollutant/g fuel)

Since the EU Sulphur Directive applies to the area included in this research, the limit value of 0.1% sulphur content was taken into account when calculating the SOx EF [37]. Emissions of PM are a function of fuel sulphur content, where it is assumed that 97.753% of the sulphur in the fuel is converted to SOx and the rest to sulphate/sulphite aerosol, classified as a part of PM [12]. That is why both S and SFC had to be determined and applied inside Equation (6) to estimate PM10 EFe. Assuming that 92% of PM10 is actually PM2.5, Equation (7) was used [12].

$$\text{PM10 EFe} = 0.23 + SFC \times 7 \times 0.02247 \times (S - 0.0024) \tag{6}$$

$$\text{PM2.5 EFe} = \text{PM10} \times 0.92 \tag{7}$$

Emissions of NOx, CH4, CO, and NMVOCs vary depending on engine load; therefore, only values for low-load adjustment were used as stated before, without conversion of EF applied for CO_2, SOx, and PM. A set of EFs values for CO and NMVOCs described in the third IMO GHG study are applied, while for CH4, new insights presented in the fourth GHG Study were implemented [12,35]. This applies particularity to LNG fuel used by different marine engines [12]. The values of EFs for NOx emitted by diesel engines are limited by a three-tier system defined in IMO MARPOL Annex VI Regulation 13 (IMO, 2013b), where the EF of each tier is subdivided in relation to engine speed and construction

date [38]. Since the NOx control requirements apply to installed marine diesel engines with an output power of more than 130 kW, values from the regulation corresponding to the technical data of ships were used as the NOx EFs in this research.

3. Results

The model performed an estimation of ship-related emissions based on relevant technical details and 49,540,895 AIS reference points that were previously processed with the aim of defining individual movement trajectories with respective operating modes and EFs. By combining the presented bottom-up logic with a relevant energy-based method, the model was able to produce high-density estimates of air pollutants released by individual ships for every port visit in 2019. Emission estimates for each port visit with all relevant features of individual ships are stored and can be handled by the model to generate various analytical results.

According to the processed data from AIS, the number of ships calling at the Port of Split—City port basin in 2019 was 16,429. This number corroborated the port traffic statistics, since the movement trajectories, such as datasets that represent port visits, form the basis for calculating emissions. The quantity of calls identified was found to match maritime transportation data with 100%, 98%, 95%, 96%, and 94% for all types of cruise ships, both types of Ro-Ro ferries, high-speed craft, tugs, and fishing ships, respectively. However, the arrival figures for excursion ships, pleasure craft and sailing ships were reported differently in the various sources of shipping statistics data and could not be compared as the other ship types. There is, therefore, a possibility that the emissions released by the mentioned ship types are greater than estimated in this research. The explanations for the discrepancies mentioned are explained in the section Uncertainties, while the distribution of port calls per ship type determined from the AIS database used in this research is shown in Figure 4.
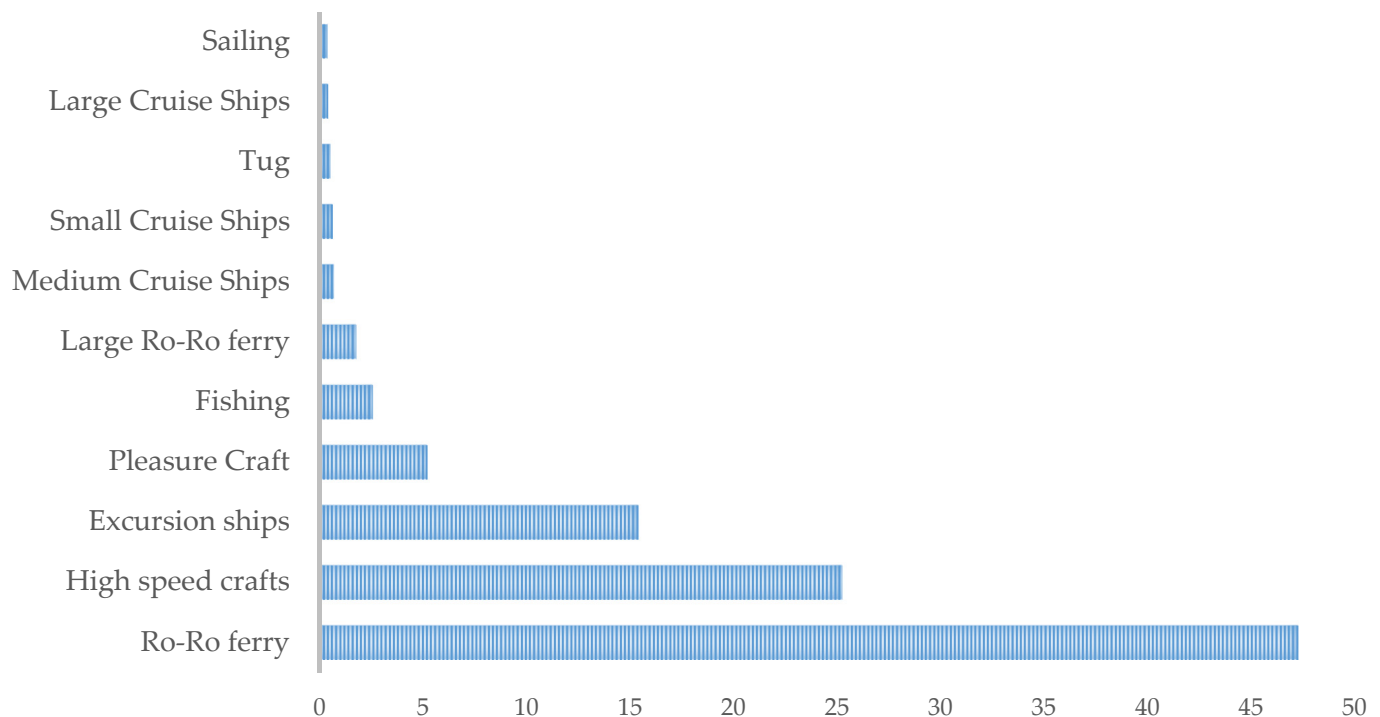

Figure 4. Share of visits to the Port of Split—City port basin in 2019 based on AIS data.

On all included ships, the most common engine type installed is a MS D engine (78%), followed by a HS D (22%) and a LS D (3%). GTU, STU, and DF are fitted on less than 1% of ships and therefore have no significant impact on emissions in the research area. With regard to the presented overview of engine details and the application of the EU Sulphur Directive, it is assumed that the entire fleet uses MDO/MGO with the limit value of 0.1% sulphur content during the entire port call.

3.1. Gas Emissions Quantification

The model was used to create an inventory of air pollutants generated by ships in the defined port area by summing the emissions from each movement trajectory for each ship, then for specific types of ships, and finally for the entire fleet. The annual emissions quantified with the model for the Port of Split—City port basin in 2019 are presented in Table 2 as totals for each ship type and released gas. In the comparison, the emissions per ship type match the distribution of port visits only for Ro-Ro ferries and high-speed craft, while a significant deviation can be observed for the other groups. The reason for this lies in the technical requirements of the propulsion and generator systems on board and the different energy demand of the individual ship types.

Table 2. Annual emissions quantified by the model for the Port of Split—City port basin in 2019 expressed in mt.

Ship Type	GHG		APS					
	CO_2	CH4	SOx	NOx	PM10	PM2.5	NMVOC	CO
Ro-Ro ferry	19,734.524	0.345	11.694	297.449	6.484	5.966	16.857	12.132
High-speed craft	5962.247	0.105	3.533	85.349	1.945	1.789	5.475	5.037
Large Ro-Ro ferry	4697.735	0.088	2.782	86.684	1.619	1.490	4.085	0.698
Large cruise ships	4276.095	0.080	2.532	77.546	1.471	1.354	3.617	0.772
Medium cruise ships	4160.025	0.077	2.464	75.264	1.427	1.313	3.509	0.821
Excursion ships	1431.938	0.033	0.849	26.338	0.526	0.484	1.870	0.836
Small cruise ships	1156.656	0.020	0.685	16.751	0.378	0.348	0.899	0.838
Pleasure craft	525.652	0.013	0.312	11.866	0.203	0.187	0.777	0.173
Fishing	351.700	0.007	0.208	4.610	0.117	0.108	0.350	0.331
Tug	135.243	0.003	0.080	1.770	0.049	0.045	0.167	0.141
Sailing	30.074	0.001	0.018	0.739	0.011	0.010	0.038	0.007
Totals	42462	1	25	684	14	13	38	22

The effects of the different groups of ships on air pollution in the port area are therefore shown in Figure 5. By examining presented overall impact of specific ship types, it can be noted that Ro-Ro ferries contributed an average of 47% of all estimated emissions, while the average share of gases released by high-speed craft is 15%. Large Ro-Ro ferries and large- and medium-sized cruise ships have a general share of 10%, while all other ship types combined are commonly below 10%, leading to the conclusion that their impact on air pollution is of limited importance.

However, the connotations of GHG and APS emissions should be considered separately, as the first group has a global impact on climate change, while the second group poses a direct threat to human health on local scale [39].
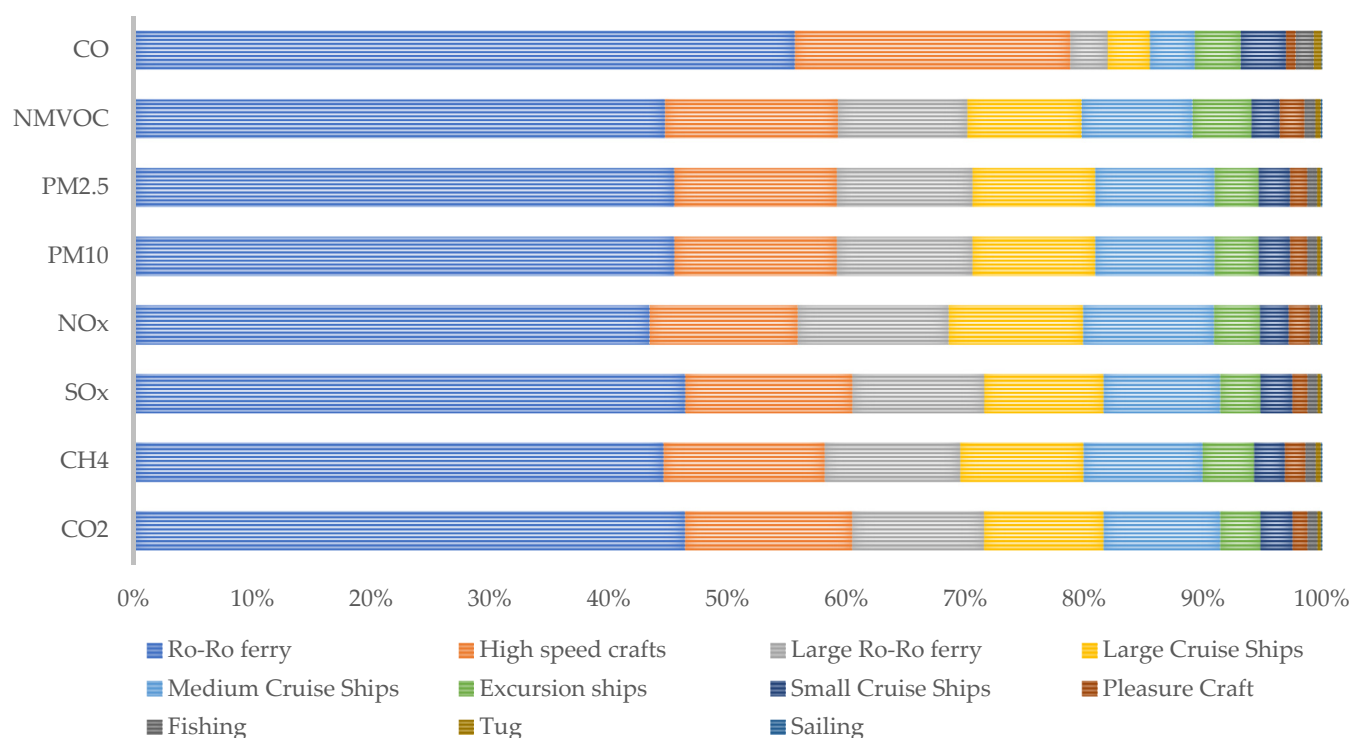
Figure 5. Proportions of emissions produced by different ship types.

3.1.1. Greenhouse Gases (GHGs)

The reason why CO_2 is the predominant GHG in the port area, with a share of more than 99.99%, is due to the almost exclusive use of MDO/MGO by the fleet, which is primarily powered by diesel engines. The amounts of CH4 released annually are therefore insignificant but could increase given the global trend towards the introduction of LNG-powered ships. As depicted in Figure 5, the GHG emissions of Ro-Ro ferries are roughly equivalent to those of High-speed craft, large Ro-Ro ferries, and medium and large cruise ships combined. To mitigate annual CO_2 emissions in the relevant area of the City port basin, the focus should therefore be on operational and technical measures aiming to increase the energy efficiency of ships which contribute most to GHG pollution.

3.1.2. Air Pollutant Substances (APSs)

At 86%, the amount of NOx emitted by ships accounts for the largest share of the total APS released. The cause for the larger NOx levels could be in the engine speed and the age of the fleet, which are particularly high in the most active ship types. Mentioned engine details are directly related to the tier system, which assumes larger EFs, resulting in the amount of emissions stated. The modernisation of liners and the introduction of exhaust gas reduction technologies such as selective catalytic reduction would be beneficial to mitigating overall NOx levels. Annual total of SOx is not severe since the 0.1% sulphur content was applied in the estimation process. However, the specified limit was based on an assumption that entire fleet used low-sulphur fuel for the entire period of arrival, berth, and departure. However, according to the EU Sulphur Directive, fuel changeover is mandatory only after arrival at berth, and since data on the content of the fuel used was limited, it is possible that SOx emissions are higher than estimated through the model [37]. The same conclusion can be drawn for PM 2.5 and PM 10 emissions, as it is assumed that sulphur not converted to SOx is released as PM [12]. As products of incomplete combustion of fuel, both CO and NMVOC are part of the total APS emissions. The estimated NMVOC values correlate with the predominant passenger ship types found in the research area, as this pollutant is generally produced primarily by evaporation from takers [40]. Higher CO emissions, especially for Ro-Ro ferries, can be explained by longer periods of low-load

operation associated with the partial combustion process, which indicates the application of a higher EF in the estimation [12].

3.2. Operating Modes and Spatial Distribution

A general overview of the emissions produced in the different operating modes indicates that 59%, 8%, and 33% were released in cruising, manoeuvring, and hoteling activity, respectively. However, this fact varies considerably with the different types of ships, which is shown in Figure 6. On an annual basis, Ro-Ro ferries, high-speed craft, excursion ships, pleasure craft, and sailing ships emitted most of the pollutants during cruising activity. On the other hand, all types of cruise ships and large Ro-Ro ferries produced larger volumes of emissions during the hoteling phase, while for tugs, the manoeuvring mode was dominant.
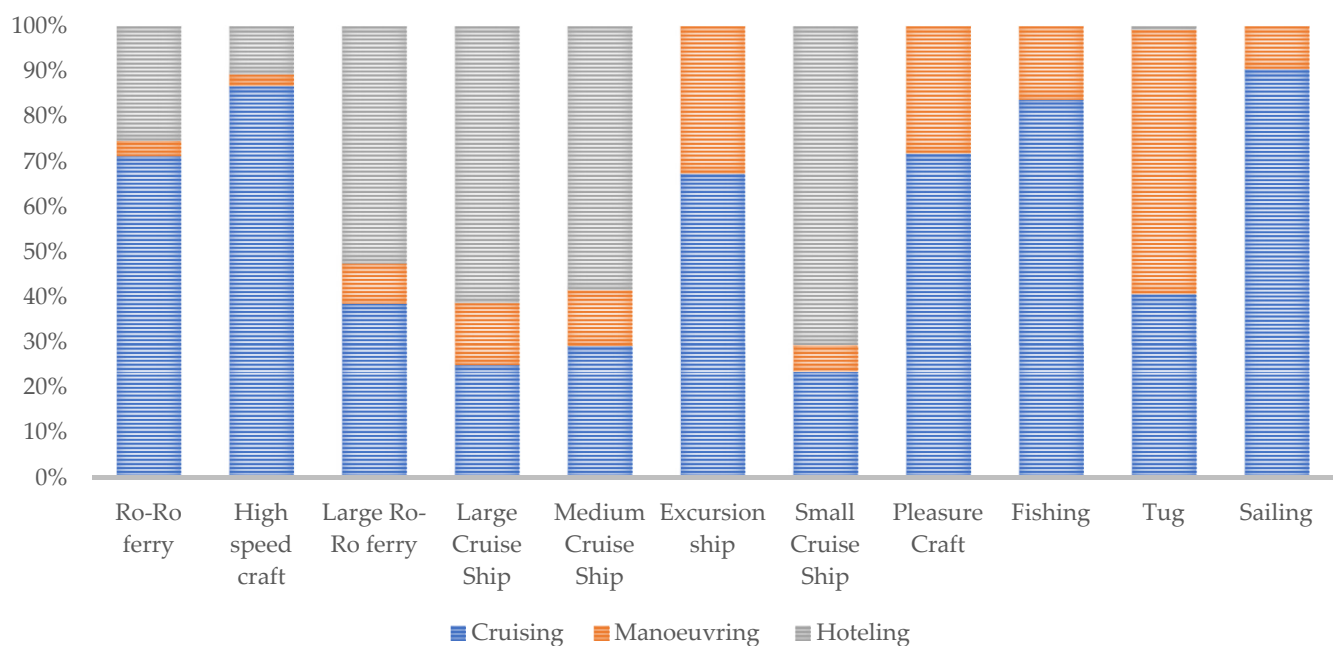

Figure 6. Distribution of quantified emissions released in different modes of operation by ship types on an annual basis.

This insight is particularly valuable for future mitigation planning based on characteristics associated with a particular operating mode. It is also important to note that APSs emitted near urban areas have a greater impact on local air quality. That is why the model was used to produce the unique high-density spatial distribution of emissions based on activities to provide an overview of the main air pollution dispersion points quantified on an annual basis for each type of ship, as is depicted in Figure 7. The figure shows that 59% of emissions released in cruising activity are within a radius of 13 NM, while 41% (manoeuvring and hoteling emissions combined) are mostly concentrated in an area with a maximum distance of 0.5 NM from the city centre.

The divergence found between the points of emission generation for different modes for Ro-Ro ferries and large cruise ships is shown in Figure 8 with a radius of 1 NM from the spot where most emissions are released. This map shows even more detailed information about the air pollutants released, as it displays the total values for each visit with a colour scale, where green stands for lower emissions and red for higher emissions, revealing the proximity of air pollution production points to the populated area. In addition to the aforementioned difference between emission production in various modes, the variance in the emission quantities released by two types of ships is also shown. For example, the legend in the top right corner of the map suggests that large cruise ships released anywhere

from 35 to 45 mt of air pollutants in hoteling, while Ro-Ro ferries released 1.2 mt while operating in cruising mode.
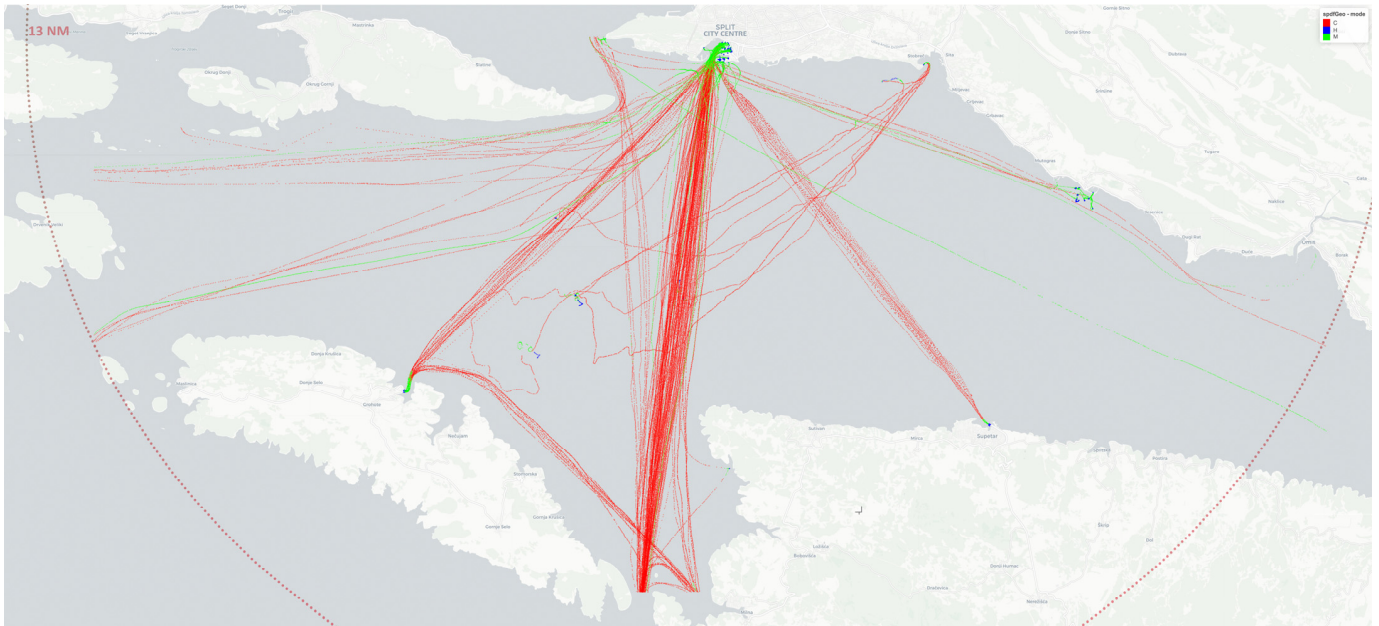

Figure 7. Activity-based ship emissions spatial distribution map. As can be seen from the activity-based ship emissions spatial distribution map, the distances between the emission dispersion points and the populated area are not great. All cruising dispersion points marked in red colour are located within a radius of 13 NM from the city centre, while most of them start at a distance of 11.5 NM and 9 NM. The proximity to the urban area applies in particular to the emissions released in the manoeuvring and hoteling phases, displayed in green and blue, respectively, as they are concentrated in an area with a maximum distance of 0.5 NM from the city centre.
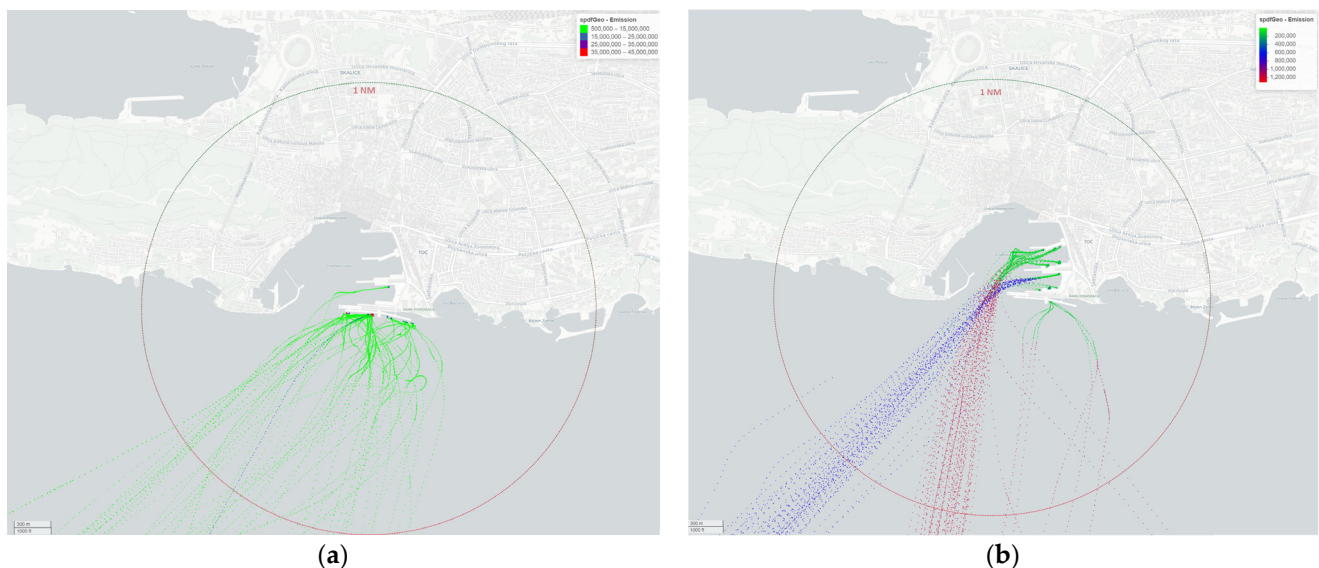

Figure 8. Activity-based ship spatial distribution map of emission sums (in g) per port call for a period of one month (October) with radius of 1 NM from the point where the largest levels of emissions are released: (**a**) large cruise ships, (**b**) Ro-Ro ferries.

3.3. Temporal Distribution—Seasonality

The increased demand for shipping services is strongly connected to the tourist season, as this industry is a major source of income for the local economy. Therefore, a higher volume of emissions was generated during the summer months, which correlates with seasonal traffic intensity. Since the different types of passenger vessels are predominant in the transportation mix, both GHG and APS production show almost the same trend, so their temporal distribution over the twelve-month period with annual average for 2019 is shown in Figure 9. It can be observed that there is a particular difference between months in which the average emissions were significantly exceeded and those in which they were approximately the same or lower. In this case, the months in which the recorded values are above average individually had emissions more than twice as high as months from the rest of the year. This difference is particularly significant for July, when emissions are generally three times higher than those estimated for January, February, March, November, or December, and almost double the annual average of 3605 t.
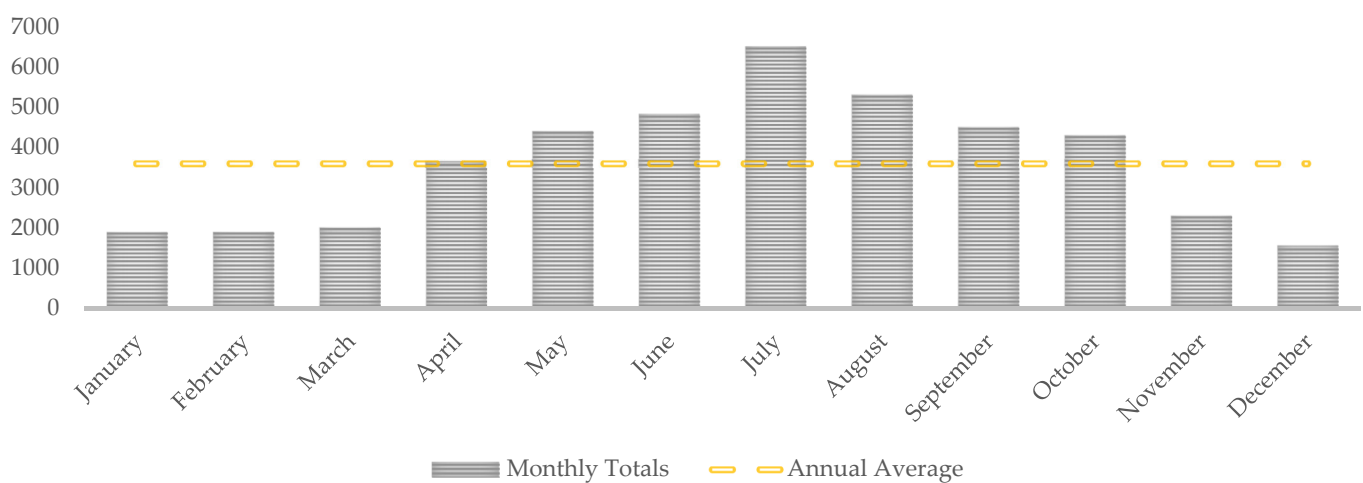

Figure 9. Temporal distribution of emission totals based on monthly fluctuations and the annual average for 2019 in mt.

Based on the analysis of intra-month variations, we propose considering two annual periods: a season when emissions are higher than the annual average and an off-season when emissions are low or close to average. Considering this, emissions are expected to increase with projected demand from tourism and shipping industry, resulting in higher concentrations of APSs in a shorter timespan, elevating the risk to the health of local population. Therefore, optimisation of emissions at peak periods should be considered, with the goal of achieving moderate values closer to the annual average.

3.4. Uncertainties

The uncertain aspects induced in this research that directly affect the level of estimated emissions are addressed in the relevant chapters. However, to provide a better overview of the unclear elements, they are examined in the following subsections.

3.4.1. AIS Data

Since the IMO Regulation V/19 states that not all ships are required to have AIS on board, a proportion of marine traffic remains invisible [1]. As this applies in particular to smaller ships that have only a minor impact on air pollution, it is assumed that the emission totals are not significantly higher. However, the technical and human errors that usually occur when the AIS is operated can lead to data loss during transmission/storage or to erroneous values which were filtered out of the database used for emission calculation. Thus, in this research, port calls estimated based on AIS data have been cross-checked with

shipping statistics databases where applicable. It is therefore possible to assume emission levels based on the difference between port calls and add them to the calculated totals.

3.4.2. Unknown Technical Details

The imputation of missing data was based on linking ships with an incomplete data set to the corresponding ship type and calculating average values for attributes with unknown information. This procedure was applied to all ships whose technical data were incomplete. Since the databases used in this research contained, on average, less than 10% of unknown information on technical characteristics per ship type and a specific differentiation of ship types was made, the imputed data show little differentiation.

3.4.3. LFs

While the LFs of the MEs were calculated on the basis of the propeller law, the same method was not applicable for estimating the workload of generators. As there was no research or database that would provide values on LFs of AEs operated in interest area, static values from several large-scale studies and papers with similar traffic and space specifications were used for the workload values of the AEs.

3.4.4. Fuel Composition

Even when the fuel type used by ships in the navigating area is known, the composition of the fuel may vary for each supply of the same product. Therefore, fuel composition assumptions were made based on the regulations in force in the research area and the details of the engine.

3.4.5. EFs

As the most complex feature that is dependent on both technical and movement characteristic, EFs can be described as the component with the highest level of uncertainty. Since the specific research on EFs involving accurate data on the engine details, fuel composition, and its consumption or workload in specific mode was not conducted on the ships operating in the research area, the EFs values have been calculated on the basis of comprehensive methods applied to the collected data.

3.4.6. Weather Conditions

Sea and air temperature, wind, currents, and wave force and direction can significantly affect fuel consumption/engine load, leading to a change in EF values and consequently emissions released by the ship. As the vessels operating in the area included in this research do not navigate in extreme weather, the influence of the mentioned conditions is limited. Also, LF values for AEs are assumed based on temperature fluctuation between warmer and colder periods, which is specifically important for passenger ships [4]. However, in future work, and for different areas, the model should include meteorological data.

4. Discussion

The annual inventory of emissions released by ships in the relevant port area, produced by the model developed in this research, provided an overview of technical, temporal, spatial, and operational aspects. Presented results are based on calculations applying relevant methodologies to a large AIS database and detailed technical data, and thus can be used for establishing broad guidelines for emissions management in port.

However, mentioned insights have a general standpoint and as such do not include the aspect of equivalence between the emission-related characteristics of different ships or port areas. For example, Ro-Ro ferries were identified as the ships that emit the greatest amount of air pollutants overall, especially when operating in cruising mode. To achieve this, they had to account for almost 50% of the total port visits. On the other hand, large cruise ships released more than four times less emissions, most of them in the hoteling phase, but only for a fraction of the total arrivals. The difference in emission production and

quantities also varies with the observed period and changes the proportion of air pollutants released between the ships. In order to introduce strategies for control of the emissions, all aspects must therefore be examined and considered, which can be a computational and time-consuming process as large databases and connections between different factors need to be analysed.

Furthermore, the volumes of calculated emissions are not comparable, even for the same ports, as the inventories often apply different methods and datasets for emission calculations [15]. A comparison of the gas volume would therefore not describe the relationship between the measurements in a meaningful way [15]. Even if the same method was used in the same area of interest, all factors and datasets used for the calculations must be consistent in order to obtain comparable emission results [15]. The most obvious examples of the discrepancies mentioned can be found in the values for gas types, ship types, EFs, LFs, or transit distances [15].

The lack of specified comparability between ships and ports is common in emissions inventories aggravates the process of an appropriate assessment of insights into the production and effects of air pollution from ships [15]. Therefore, the introduction of a scalable system based on the analysis of emissions-related data from inventories could provide a more transparent and efficient overview of the important characteristics of air pollution from ships and port areas. The application of the above system may serve as a coherent framework for the control of air quality in port communities.

Since the model presented in this research already integrates a large database of emission features with calculated results, it is possible to extend its capabilities by including a comparison logic in future work.

5. Conclusions

In this research the analytical model for estimation of ship-sourced emissions was developed and used to produce an inventory of combustion gases released in the area relevant to the Port of Split—City port basin for 2019. To estimate emissions of GHGs and APSs, technical details and ship movement data from AIS were integrated inside the model where bottom-up logic with an energy-based method was applied. Therefore, to obtain a high-density overview of emissions, the modelling was carried out using three main interconnected components.

First was the preprocessing segment, where the technical and AIS datasets were prepared by applying conversion, cleansing, filtering, formatting, and merging techniques to create the specific data arrangement of features relevant to the ship-based emission estimation.

In the second, the processing component, unique categories of ship types were defined based on different classifiers to ensure a more accurate and effective imputation of missing data, while also providing the background for a future extension of the model's predictive capabilities. Estimates were then made of the GHG and APS quantities released for all ships recorded in the AIS database for the year 2019 within the research area.

Finally, the results produced by the model show that 42462, 1, 25, 684, 14, 13, 38, and 22 mt of CO_2, CH4, SOx, NOx, PM10, PM2.5, NMVOC, and CO were emitted from ships in the relevant area of the Port of Split—City port basin, respectively. It was noted that most annual emissions are generated during the tourist season, as this period has the highest frequency of port calls. Because of the high arrival rate, Ro-Ro ferries were identified as the ship type that emitted the largest amount of air pollutants, while C activity was the dominant mode of operation for emission production overall.

Emission estimates with all datasets containing information on characteristics that are important for the production of air pollutants are stored and can be handled by the model to generate various analytical results. Therefore, the model was able to produce detailed inventory and reports with various statistical features that can be used by experts and decision-makers for managing emissions in port areas. Furthermore, as the structure

of the model's components is flexible and an adaptable approach to database imputation is taken, it is possible to extend its potential by pursuing the following:

- Modelling emission estimates for different port areas by integrating location-specific AIS data and technical details of related ships.
- Applying new insights, mainly named in the chapter on uncertainties, to the production of combustion gases from marine engines with the aim of obtaining even more accurate calculations.
- Introducing a scalable system to provide a more transparent and efficient overview of the important characteristics of air pollution from ships and port areas.
- Extending predictive capabilities by relying on large shipping databases to create scenarios for the future development of air pollution from the fleet in a specific port area.

References

1. IMO. Available online: https://www.imo.org (accessed on 11 October 2023).
2. ICCT. Available online: https://theicct.org (accessed on 11 October 2023).
3. UNCTAD. Available online: https://unctad.org (accessed on 11 October 2023).
4. Tzannatos, E. Ship Emissions and Their Externalities for the Port of Piraeus—Greece. *Atmos. Environ.* **2010**, *44*, 400–407. [CrossRef]
5. EMSA. Available online: https://www.emsa.europa.eu/ (accessed on 11 October 2023).
6. WARTSILA. Available online: https://www.wartsila.com/ (accessed on 11 October 2023).
7. Nunes, R.A.O.; Alvim-Ferraz, M.C.M.; Martins, F.G.; Sousa, S.I.V. Assessment of Shipping Emissions on Four Ports of Portugal. *Environ. Pollut.* **2017**, *231*, 1370–1379. [CrossRef] [PubMed]
8. WHO. Available online: https://www.who.int (accessed on 21 October 2023).
9. Sofiev, M.; Winebrake, J.J.; Johansson, L.; Carr, E.W.; Prank, M.; Soares, J.; Vira, J.; Kouznetsov, R.; Jalkanen, J.-P.; Corbett, J.J. Cleaner Fuels for Ships Provide Public Health Benefits with Climate Tradeoffs. *Nat. Commun.* **2018**, *9*, 406. [CrossRef]
10. IMO. Available online: https://www.imo.org/en/ourwork/environment/pages/air-pollution.aspx (accessed on 21 October 2023).
11. IMO. Available online: https://www.imo.org/en/ourwork/environment/pages/ghg-emissions.aspx (accessed on 21 October 2023).
12. International Maritime Organization. *Fourth IMO GHG Study*; International Maritime Organization: London, UK, 2020.
13. United Nations Conference on Trade and Development. *Review of Maritime Transport*; United Nations: New York, NY, USA, 2021.
14. ESPO. Available online: https://www.espo.be/publications (accessed on 25 October 2023).
15. Bojić, F.; Gudelj, A.; Bošnjak, R. Port-Related Shipping Gas Emissions—A Systematic Review of Research. *Appl. Sci.* **2022**, *12*, 3603. [CrossRef]
16. IPCC. Available online: https://www.ipcc.ch/ (accessed on 25 October 2023).
17. EEA. Available online: https://www.eea.europa.eu/publications/emep-eea-guidebook-2023 (accessed on 25 October 2023).
18. EC. Available online: https://climate.ec.europa.eu/index_en (accessed on 5 November 2023).
19. UNFCCC. Available online: https://unfccc.int/documents/627738 (accessed on 5 November 2023).
20. DZS. Available online: https://podaci.dzs.hr/ (accessed on 5 November 2023).
21. MMPI. Available online: https://mmpi.gov.hr/ (accessed on 5 November 2023).
22. Lee, H.; Pham, H.T.; Chen, M.; Choo, S. Bottom-Up Approach Ship Emission Inventory in Port of Incheon Based on VTS Data. *J. Adv. Transp.* **2021**, *2021*, 5568777. [CrossRef]
23. Chen, D.; Zhao, Y.; Nelson, P.; Li, Y.; Wang, X.; Zhou, Y.; Lang, J.; Guo, X. Estimating Ship Emissions Based on AIS Data for Port of Tianjin, China. *Atmos. Environ.* **2016**, *145*, 10–18. [CrossRef]
24. Tichavska, M.; Tovar, B. Port-City Exhaust Emission Model: An Application to Cruise and Ferry Operations in Las Palmas Port. *Transp. Res. Part A Policy Pr.* **2015**, *78*, 347–360. [CrossRef]

25. Lee, H.; Park, D.; Choo, S.; Pham, H.T. Estimation of the Non-Greenhouse Gas Emissions Inventory from Ships in the Port of Incheon. *Sustainability* **2020**, *12*, 8231. [CrossRef]
26. Song, S. Ship Emissions Inventory, Social Cost and Eco-Efficiency in Shanghai Yangshan Port. *Atmos. Environ.* **2014**, *82*, 288–297. [CrossRef]
27. Schwarzkopf, D.A.; Petrik, R.; Matthias, V.; Quante, M.; Majamäki, E.; Jalkanen, J.P. A Ship Emission Modeling System with Scenario Capabilities. *Atmos. Environ. X* **2021**, *12*, 100132. [CrossRef]
28. Starcrest Consulting Group. *Port of Long Beach Air Emissions Inventory—2010*; Starcrest Consulting Group: Poulsbo, DC, USA, 2010.
29. LUS. Available online: https://portsplit.hr/ (accessed on 8 November 2023).
30. Bošnjak, R.; Šimunović, L.; Kavran, Z. Automatic Identification System in Maritime Traffic and Error Analysis. *Trans. Marit. Sci.* **2012**, *1*, 77–84. [CrossRef]
31. Fournier, M.; Casey Hilliard, R.; Rezaee, S.; Pelot, R. Past, Present, and Future of the Satellite-Based Automatic Identification System: Areas of Applications (2004–2016). *WMU J. Marit. Aff.* **2018**, *17*, 311–345. [CrossRef]
32. Marine Insight. Available online: https://www.marineinsight.com/ (accessed on 8 November 2023).
33. IALA. Available online: https://www.iala-aism.org/ (accessed on 8 November 2023).
34. Starcrest Consulting Group. *San Pedro Bay Ports Emissions Inventory Methodology Report—Version 2*; Starcrest Consulting Group: Poulsbo, DC, USA, 2021.
35. International Maritime Organization. *Third IMO GHG Study*; International Maritime Organization: London, UK, 2015.
36. Marine Environment Protection Committee. *RESOLUTION MEPC.308(73)—ANNEX 5*; International Maritime Organization: London, UK, 2018.
37. The European Parliament and the Council. *Directive (Eu) 2016/802*; The European Parliament and The Council: Luxembourg, 2016.
38. Marine Environment Protection Committee. *MEPC.177(58)*; International Maritime Organization: London, UK, 2008.
39. European Commission. Available online: https://ec.europa.eu/ (accessed on 12 November 2023).
40. IPCC. Available online: https://archive.ipcc.ch/ (accessed on 12 November 2023).